Applied Physics Research; Vol. 6, No. 5; 2014
ISSN 1916-9639 E-ISSN 1916-9647
Published by Canadian Center of Science and Education

Investigation of Hot Cathode and Hollow Anode of Argon Glow Discharge Plasma

Shamoo K. Al-Hakary[1], Luqman Dosky[2] & Shamil K. Talal[1]

[1] Physic Department, Faculty of Sciences, Zakho University, Iraq

[2] Physic Department, Faculty of Sciences, Duhok University, Iraq

Correspondence: Shamoo K. Al-Hakary, Physic Department, Faculty of Sciences, Zakho University, Iraq. E-mail: shamookhudaida@yahoo.com

Received: June 23, 2014 Accepted: July 24, 2014 Online Published: August 21, 2014

doi:10.5539/apr.v6n5p45 URL: http://dx.doi.org/10.5539/apr.v6n5p45

Abstract

Hot cathode and hollow anode argon DC glow discharge plasma at different pressures of (0.04, 0.05, 0.06, 0.07, 0.09, 0.2, 0.4, and 0.8 mbar) has been investigated. The experiments were carried out under the influence of pressure and filament cathode current on voltage – current characteristics of glow discharge and its breakdown voltage. Plasma parameters have been measured and obtained using single probe method at fixed discharge current (I_d=1.88 mA) and hollow anode diameter. A computer MATLAB program is performed for this purpose. It was shown that the discharge voltage – current characteristics curve has a positive resistance and represents an abnormal glow region at pressure (0.04 and 0.06) mbar for different filament current. The breakdown voltage increases as the filament current is increased. In different pressure, electron temperature shows different behavior with increasing filament current. Electron density varies nearly inversely with the filament current, but it is increase due to increase of pressure from (1 to 3 mbar), then tends to decrease for the higher pressure. There are two groups of electrons according to the two peaks of (EEDFs), and the peaks amplitude decrease, with the increases of both filament current and gas pressure.

Keywords: hot cathode, hollow anode, argon glow discharge, plasma parameters

1. Introduction

The detail of a gas discharge by a hot filament cathode has been studied by many researchers, Ehlers and Leung (1979) had investigated the electron emission from filament cathodes in gas discharge, and shown magnetic field produced by the filament heating current cause inhomogeneous emission of electron concentration of discharge current at a localized position of a filament. Hot cathode discharge plasma with negative ions is widely used in fusion researches and development and in modern plasma processing technologies (Cercek & Gyergyek, 2004). Stable operation of a cylindrical hall thruster has been achieved by Granstedt, Raitses, and Fisch (2008), using a hot wire cathode, which functions as a controllable electron emission source. Miyamoto, Imakita, Kasuya, Shimamoto, and Wada (2009) directly heated high temperature cathodes of refractory metals such as tungsten run electric current of more than several tens of amperes. The electric current makes magnetic field around the cathode wire and the magnetic field cause inhomogeneous emission of electrons from the cathode. Very low electron temperatures have been obtained by Handly and Robertson (2009), in a hot-filament discharge device by having a set of conditions designed to minimize heating of the confined electrons. Zhe, Zhigang, Yikang, and Xiaozhang (2010) generated a sheet plasma is by a mesh anode and a single hot-filament cathode with a DC power supply, and its characteristics are experimentally investigated. Flaxer (2011) produced electros through thermionic emission by heating a wire filament, accelerating the electrons by high voltage, and ionizing the analyzed molecules. Yasserian, Borkhari, and Dorranian (2012) investigate the characteristics of a DC electrical breakdown accompanied with a hot tungsten filament. The device includes two flat electrodes and a moveable filament which is located behind the cathode. The left-hand of the Paschen curve is obtained for different of the currents of the filament as well as various locations in the presence of argon and nitrogen gases. Chen and Jiang (2013) show that the difference of hot cathode operation mode has a great influence on the arc discharge of high current ion source. Borkhari and Yasserian (2013) studied the influence of a hot filament on the electrical breakdown characteristics for different ratios of argon and nitrogen gases for a wide range of pressure.

On the other hand, hollow anode discharge can be more widely applied; it can be used, in ion-electron sources and spectroscopy, when the hollow anode discharge is established very bright plasma is formed in the hollow anode. Matsuura and Wagatsuma (2013) employed Glow discharge optical emission spectrometry (GD-OES) for the direct analysis of solid samples, because sample atoms are directly introduced into the plasma through cathode sputtering. A Grimm-style glow discharge excitation source, whose hollow anode had an inner diameter of 8 mm, was employed as the excitation source. Mujawar (2013) deal with the study of oxygen negative ion formation in the anodic glow plasma. The anodic glow is characterized by a double layer having a steep gradient in T_e and electron density. The anodic glow is created via D.C discharge between a hollow tubular-anode in conjunction with parallel plate cathodes. Tutyk, Ovcharuk, Gasik, and Maslenikov (2013) made an experimental researches of features of plasma-beam discharge (PBD) generation mode in the gas discharge electron gun operation with cold cathode and the hollow anode on the basis of the high-voltage glow discharge in a range of helium pressure $P = 10 \div 130$Pa (Abdelsalam, Abdelrahman, Soliman, Basal, & Authority, 2013). Study of optimal ion optic system for extraction of low current ion beam from plasma ion source based on glow discharge. The study based on experimental investigations and computer simulations results. Shevchenko, Tarala, Shevchenko, and Titarenko (2014) investigate an influence of the deposition conditions on the characteristics of amorphous carbon films obtained with the help of the ion source based on reflective discharge with hollow cathode. Jiang et al. (2014) present experimental results of a novel electron gun with a vacuum-arc-plasma cathode used in microwave tube devices. The plasma cathode is based on a vacuum-arc discharge with a novel hollow anode and a Pierce-type electrostatic focusing system.

The present work aims to investigate experimentally the effect of filament current on voltage – current characteristic curve of hot cathode and hollow anode argon discharge as well as its breakdown voltage V_b. Furthermore, study this effect on some plasma parameters, such as electron temperature and its density. As well as plasma potential and electron energy distribution function under different working argon gas pressure.

2. Experimental Setup

A picture of the cylindrical discharge chamber is shown in Figure 1. A cylindrical Pyrex glass tube of 5 cm diameter and 25 cm length was used. Both sides of tube are opened in order to move the electrodes through them to obtain good homogenous discharge and also to change the distance between the electrodes. Two cylindrical plastic rubbers were used to close both sides of the chamber to prevent the leakage of gas as well as to insert the electrodes through them. The distance between two electrodes was fixed to 112 mm. Tube was providing with two pipe connections, one for rotary vacuum pump and the other for single probe and gas inlet which is a capillary copper tube of 1.7 mm outer radius. Both single probe and gas inlet are mounted in the another plastic rubber as shown in Figure 1. Argon gas of high purity 99.99 was used in our experiments and Mechanical rotary pump was used [Trivac E2, Pr. Nr. 140000, Lybold], to evacuate the system to an ultimate pressure (7.5×10^{-3}) torr, this is in turn connected to discharge chamber through a piping tube, thermocouple vacuum gauge is used for measuring pressure and needle valve to control the argon gas flow. The experiments were carried out under pressure ranged from 1.5×10^{-2} to 7.5×10^{-1} torr. Figure 2 represents a schematic diagram of the discharge system.

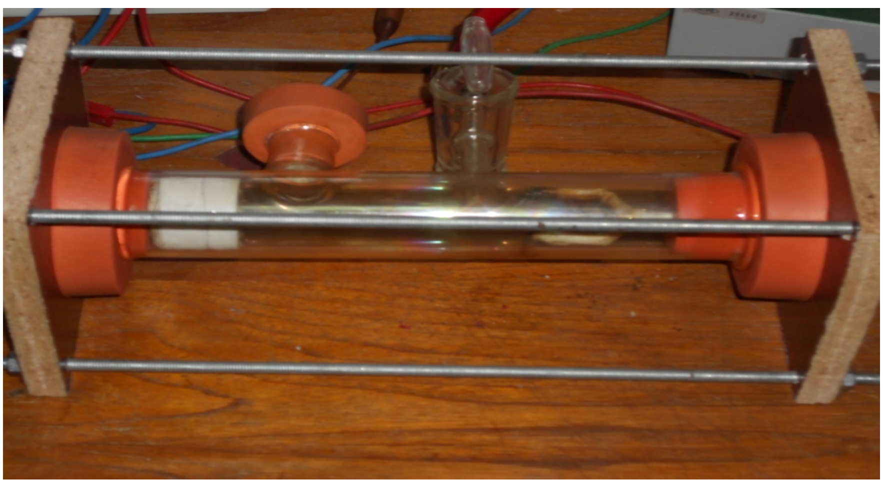

Figure 1. Picture of cylindrical discharge chamber

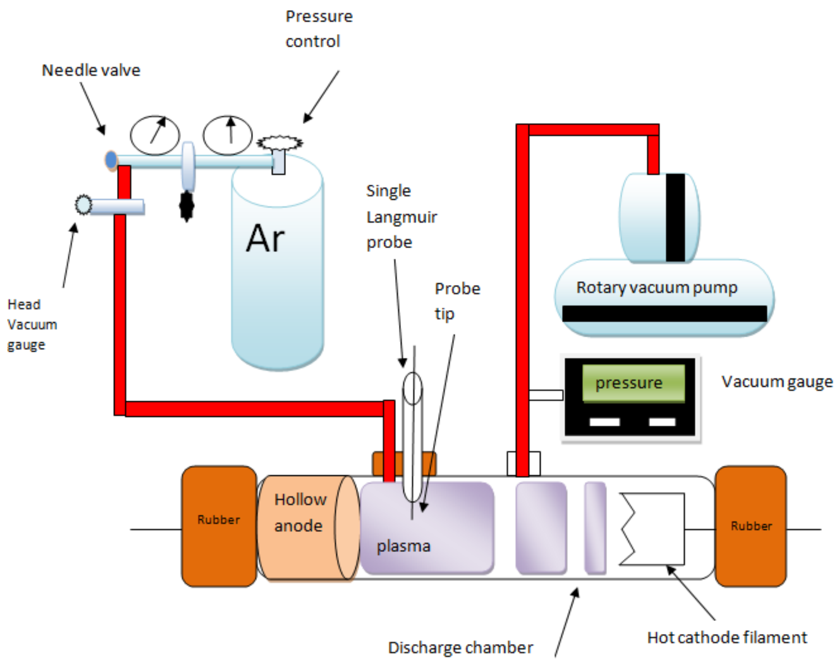

Figure 2. Schematic diagram of the discharge system

A hollow cylindrical anode of 4cm inter diameter, 3.5 cm of hollow depth and 0.5 cm thickness is made from copper metal as illustrated in Figure 3. The purpose of using this type of anode to get more stable and denser plasma at the axial of the discharge. The external area of hollow anode has been isolated by an insulator (Teflon) in order to get the discharge just inside the hole of the anode as shown Figure 3. The end of Hollow anode is connected to the external electric circuit through cylindrical plastic rubber to prevent leakage.

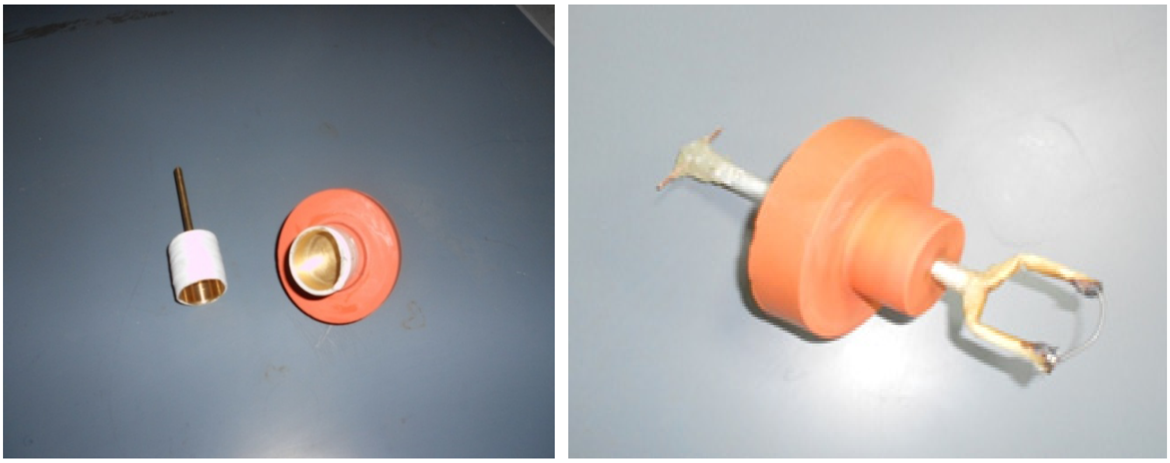
Figure 3. Cylindrical hollow anode and Cathode filament with rubber holders

Cathode filament was manufactured from (tungsten) of 1.5 cm spiral diameterand 5 cm length as shown in Figure 3. Filament was heated using a DC power supply [3B power supply U21060]. It is a variable power supply of range of (0-24) V and maximum current 20 A. In the present work the filament was heated by passing the current ranged from (0-1.5). Beyond this range the filament began to glow the system.

Single probe was constructed from tungsten wire of radius (0.1 mm) and the length of 6 mm which is exposed to discharge. This in turn, inserted to the chamber through a glass tube and the latter is entered to the positive column through the cylindrical plastic rubber. The probe was fixed within a capillary tube of glass and shielded by a plastic insulator to prevent their connection. Before each experimental measurement, Probe was cleaned by using a fine sand paper, acetone, deionizer water. Discharge voltage has been supplied to the electrodes system by a DC power supply [3B power supply U21060], of range (0-6000) V and the maximum output current (2 mA). A digital multi meter [Mastech M9803R True RMS MULTIMETER] was used to measure the discharge current (I_d). The non-linear protective resistor (lamp) was used to limit the discharge current and avoid the streamer to pass through the chamber to make the spark breakdown (Lochte-Holtegreven, 1968). This type of non-linear resistor was chosen because it provides a relatively high power of 25watt out cooling process (Salim, 2007). The probe voltage was obtained from (220 V-50 HZ), using variac and an isolated transformer (100 V-50 Hz) to bias the probe about 100 Volt as shown in Figure 4. Also a direct resistance (10 KΩ) is used to convert the voltage to real value of current through MATLAB program. The capacitor [C50 SAMER 29539] was used to reduce the phase difference in (I_p – V_p) characteristic of probe. The x-y recorder (oscilloscope) traces the (I_p – V_p) characteristic of the probes, and the voltage on the probes is recorded on the x-axis, while the current through the probes is recorded on the y-axis, as the voltage drop across the resistance of value (10 KΩ). The present work includes two different parts. The first part concerns with the influence of the filament current on the voltage - current characteristics of discharge and its breakdown voltage under different gas pressure without using single probe. For this purpose, we used the circuit shown in Figure 4 without the probe circuit. The second part include the plasma parameters measurements such as Electron temperature, electron density and plasma potential as well as (EEDFs) at various filament current using circuit shown in Figure 4.The experiment were started for two cases, firstly to evacuate the system to the required pressure under the flow of argon gas to the chamber continuously.

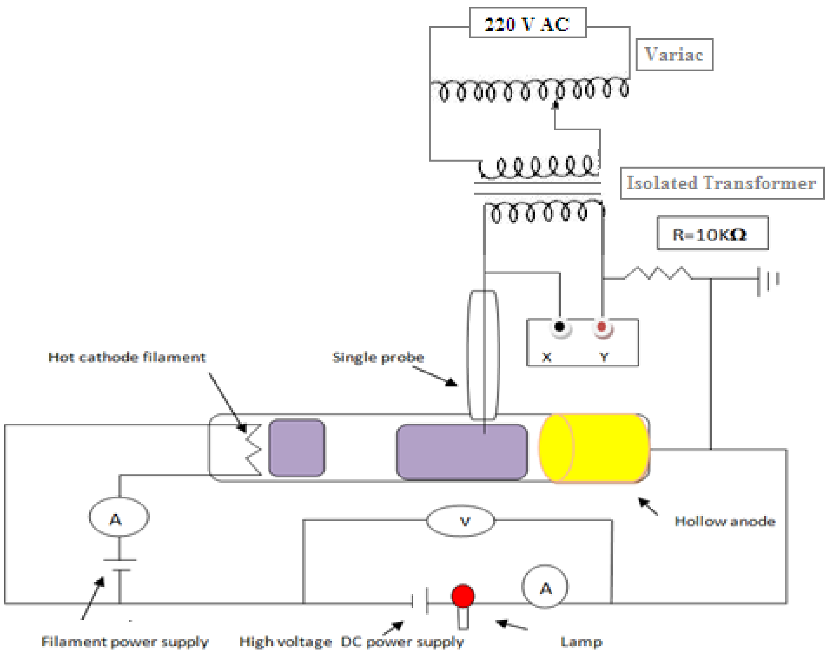

Figure 4. Discharge electric circuit

Plasma was created by applying high voltage from DC power supply sufficient for occurring breakdown of gas and obtaining an abnormal glow discharge (positive resistance) with and without the filament current ranged from (0-1.5) A for the first part to obtain the discharge characteristics and the Paschen's curve under different filament current and gas pressure. This procedure was repeated for the second part using single probe and an oscilloscope to obtain single probe characteristics. For more details see Hajy (2014).

3. Experimental Results and Discussion

Voltage-current characteristics of the discharge were obtained using voltmeter and ammeter. Figure 5 represents an abnormal glow discharge characteristics at pressure of (0.04 and 0.06) mbar for different filament currents. It is clear that an increase of the discharge voltage was accompanied by an increase of the discharge current (positive resistance). Also figure shows that increasing filament current causes shifting the characteristics towards higher discharge voltage. This latter behavior means that increasing emitted electrons from the filament enhance the negative space charge near the anode and consequently to that increasing discharge voltage as well as its resistance (Jomachi & Klobes, 2005).

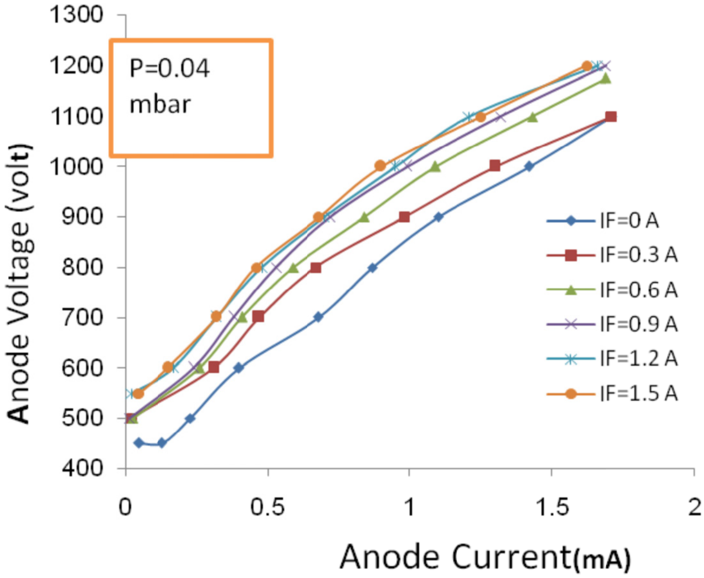

Figure 5. Voltage - current characteristics of glow discharge

Breakdown voltage as a function of filament current is represented in Figure 6 for two different gas pressures. It is obvious from the figure that the increase of emitted electron from the cathode leads to the increases of the negative space charge near the anode and the anode does not receive all the emitted electrons. The remaining electron gathers in thickening the negative space charge. Therefore, enhancing the breakdown voltage (Jomachi & Klobes, 2005).

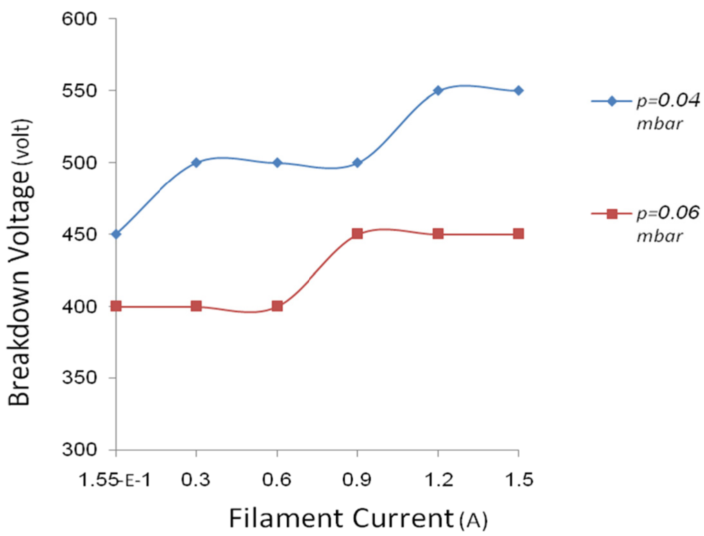

Figure 6. Breakdown voltage versus filament current

Later the breakdown voltage as a function of product of pressure and inter- distance (electrode spacing), close to the well-known Paschen's curve, Figure 7.

This behavior of Paschen's curve is a good agreement with the previous study (Eizaldeen & Ashwaq, 2012).

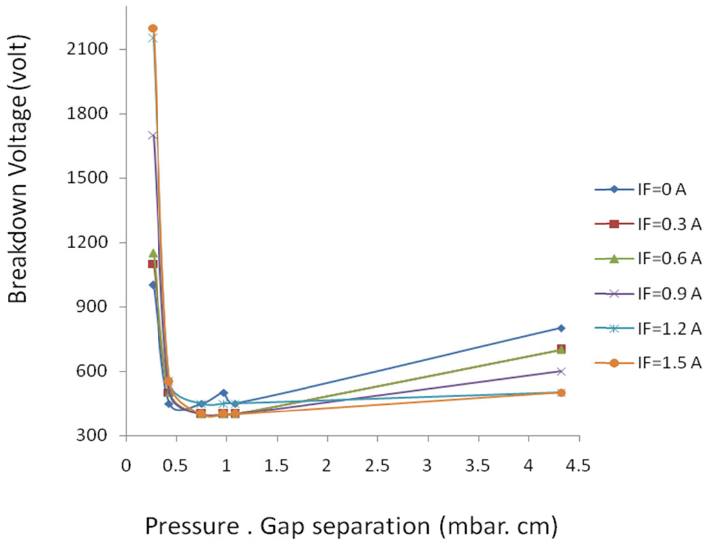

Figure 7. Paschen's curve for argon gas

In the second part of the present study, Plasma parameters have been obtained from single probes characteristics and MATLAB computer program is used to determine the electron temperature and its electron density for different pressure and filament current. The variation of electron density with the filament current, shown in Figure 8 is nearly inversely proportional, since increases of the filament current causes increases of the negative space near the anode, consequently the breakdown will be increased and the number of ionizing collisions as well as will be decrease according to that (Grill, 1993).On the other hand, the electron density increase according to the increase of pressure from (1 to 3mbar) and then tends to decrease for the higher pressure as shown in Figure 9. This range of pressure represents the left hand branch of Paschen's curve approaching to minimum point and towards a higher range of pressure that is in the right hand branch of Paschen's curve (Swarnalatha, Sravani, Gunasekhar, Muralidhar, & Mohan, 1997).

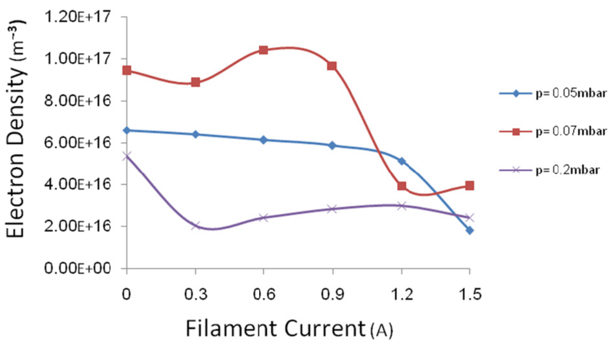

Figure 8. Electron density versus filament current

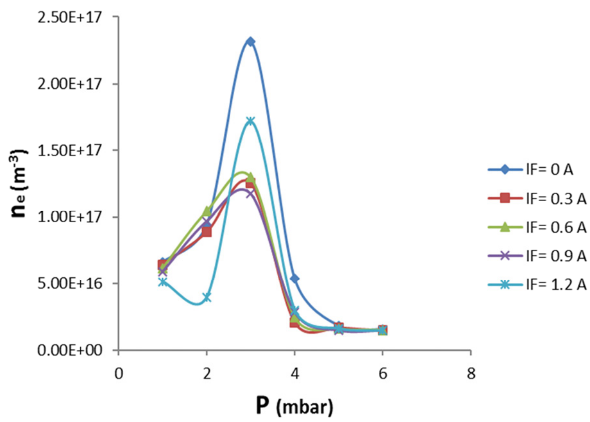

Figure 9. Electron density as a function of gas pressure

Electron temperature appears different behaviors with the increase of the filament current at the low and high pressure investigated, Figure 10. It was found that the electron temperature is increased clearly with filament current at low pressure ranged from (0.05 to 0.07) mbar .This is because of small number of neutral atoms and less collisions of electron with others plasma particles (Griener, 1998). Therefore, emitted electron from the filament can acquire energy from the applied electric field. Contrary to that, at high pressure ranged from (0.4 to 0.8) mbar, the electron temperature decrease clearly after the filament current 0.6 A. This is because the emitted electron from the cathode will lose almost its energy during the non - ionizing collisions with others plasma particles and thickening the negative space charge near the anode (Jomachi & Klobes, 2005).

Pressure dependence of electron temperature is represented in Figure 11.The most important result here is the decreasing T_e with pressure ranged from (1 to 3) mbar, appearing similar variation as the previous work (Eizaldeen & Ashwaq, 2012).Then, it tends to increase with gas pressure contrary to the regular variation of T_e versus gas pressure. At this Operating condition, the trend of $(T_e)_{high}$ is almost opposite to that of $(T_e)_{low}$ due to the difference of mechanism of electron heating process. At low pressure, the high energy electrons are actively heated by collision-less stochastic heating while the low energy electrons are confined between the bulk and sheath regions of plasma. At high pressure, on the other hand, the low energy electrons are heated by coalitional heating. As a result $(T_e)_{high}$ is decreased while $(T_e)_{low}$ is increased as the pressure is raised (Park, You, & Choe, 2010).

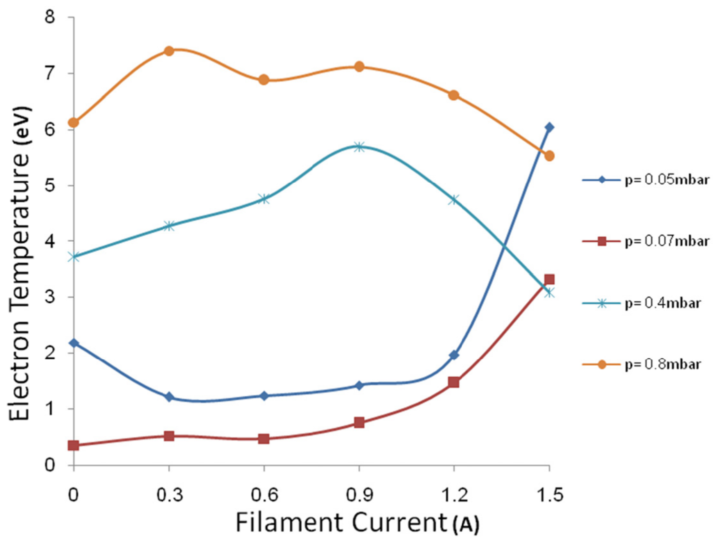

Figure 10. Electron temperature versus filament current

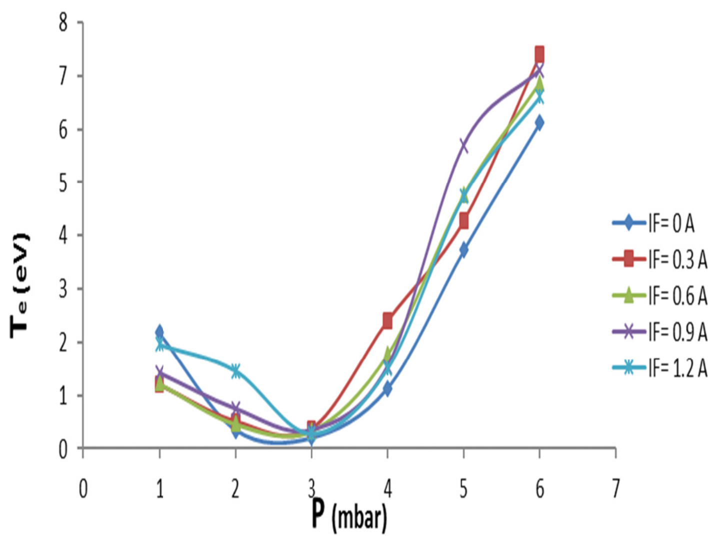

Figure 11. Electron temperature as a function of gas pressure

Plasma potential V_s is in fact the electric potential in plasma without existing probe, as well as the potential at which all electron arriving near the probe are collected and the probe current equal to electron saturation current (Grill, 1993). With respect to variation of plasma potential with the filament current, there is no significant change for different pressure. While the behavior of plasma potential with the gas pressure is a decreasing relation from the positive values at low pressures towards the negative values at higher pressures, Figure 12. The positive values are occurred at the low pressures, while the negative values are at high pressures. This latter effect is due to the change that is caused by the accumulation of heavy negative ions at the axial region of the discharge, however this effect disappears at a lower pressure (Leshkov, Kudrna, Chichina, & Pickova, 2008; Fritsche, Chevolleau, Kourtev, Kolitsch, & Möller, 2002).

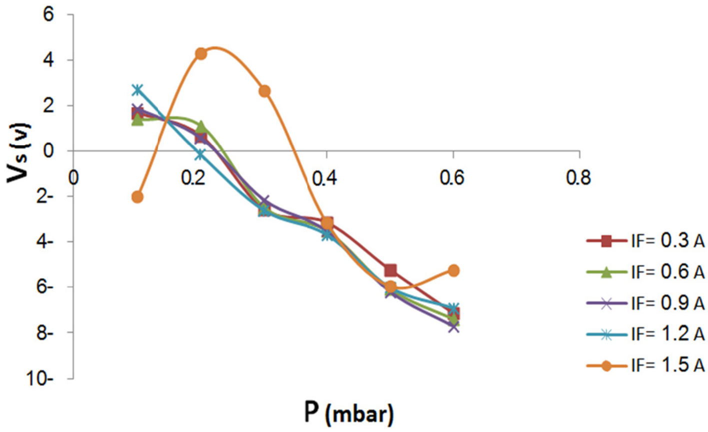

Figure 12. Plasma potential versus gas pressure

Electron energy distribution function (EEDF) in a low pressure processing discharge is a good indicator of the state of the plasma (Braithwaite, 1990). Chemical kinetics is especially sensitive to the (EEDF) and the electron population plays a central role in coupling power into the desired surface reactions. Mess development and transfer will be aided by knowledge of the (EEDF) and its sensitivity to various process parameters. Furthermore, the current-voltage characteristic of the probe represents integrated (EEDF) information which can be recovered by differentiation. The basic trick used for obtaining the (EEDF) is the exploitation of the Druyvestey formula Azooz (2008).

$$F(E) = \frac{(8mV)^{1/2}}{An\,e^{3/2}} \frac{d^2I}{dV^2} \tag{1}$$

Where m is the electron mass, e its charge and n is electron number density, A is the probe area and I and V its current and voltage respectively. According to Equation 1, one can at least obtain the (EEDF) from the evaluation of the second derivative of the single Langmuir probe (I_p-V_p) characteristics curve. A reasonable empirical equation that can describe the single probe characteristics, is an exponential transformation to a tangent hyperbolic function .We may thus write

$$I = \exp\left[a_1 \tanh\left(\frac{V+a2}{a3}\right) + a_4\right] \tag{2}$$

These Four free fitting parameters are related to plasma properties:

1) Irrespective of a_1 and a_2, and as V becomes highly negative, the tangent hyperbolic term will reach the limiting value of -1. Thus the ion saturation current will becomes :

$$I_{is} = e^{-a1} + a_2 \tag{3}$$

2) At sufficiently large positive value of V, the limiting value of the tangent hyperbolic will practically equal +1. This will give the electron saturation current

$$I_{es} = e^{a1} + a_2 \tag{4}$$

3) Solving Equation 2 for I = 0 will yield the probe floating potential

$$V_f = a_3 \tanh^{-1} [\ln(-a_4)/a_1] - a_2 \tag{5}$$

The procedure for obtaining plasma parameters is a software package in (MATLAB) language capable of carrying out all Langmuir probe analysis written by Azooz (2008). The software can be freely downloaded as a ZIP file from the (MATLAB) file exchange library. Please for more information visit to www.mathworks.com/mathcentral/fileexchange/19312-Langmuir-probe-c. The inputs to this software are the probe (I_p-V_p) data and starting guess values of the four free fitting parameters by fitting the probe (I_p-V_p) characteristics with Equation 2 as shown in Figure 13. Substitute the obtained four free parameters in to Equation 2, then find the second differentiation of the obtained equation, finally Substitute in to Equation 1 to obtain the distribution function. Output of the program is the plasma parameters.

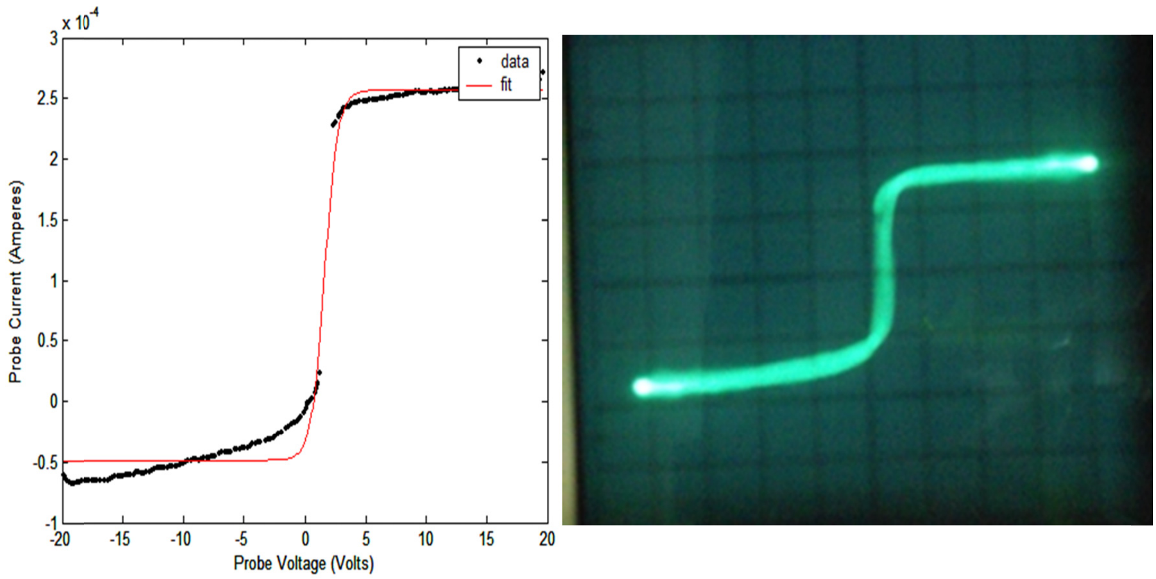

(a) $(I_p\text{-}V_p)$ Characteristics plot of data with fitting curve (b) picture of oscillogram

Figure 13. Single probe characteristics, p= 5×10^{-2} mbar and $I_f = 0$

Later the calculated EEDF from the fitting method was fitted to both Maxwell and Druyvesteyn distributions functions according to the two following equations respectively:

$$F\,(E) = 2.07(E_{av})^{-3/2}\,E^{1/2}\,exp(-1.5W/\,E_{av}) \tag{6}$$

$$F\,(E) = 1.04(E_{av})^{-3/2}\,E^{1/2}\,exp(-0.55W^2/\,E^2{}_{av}) \tag{7}$$

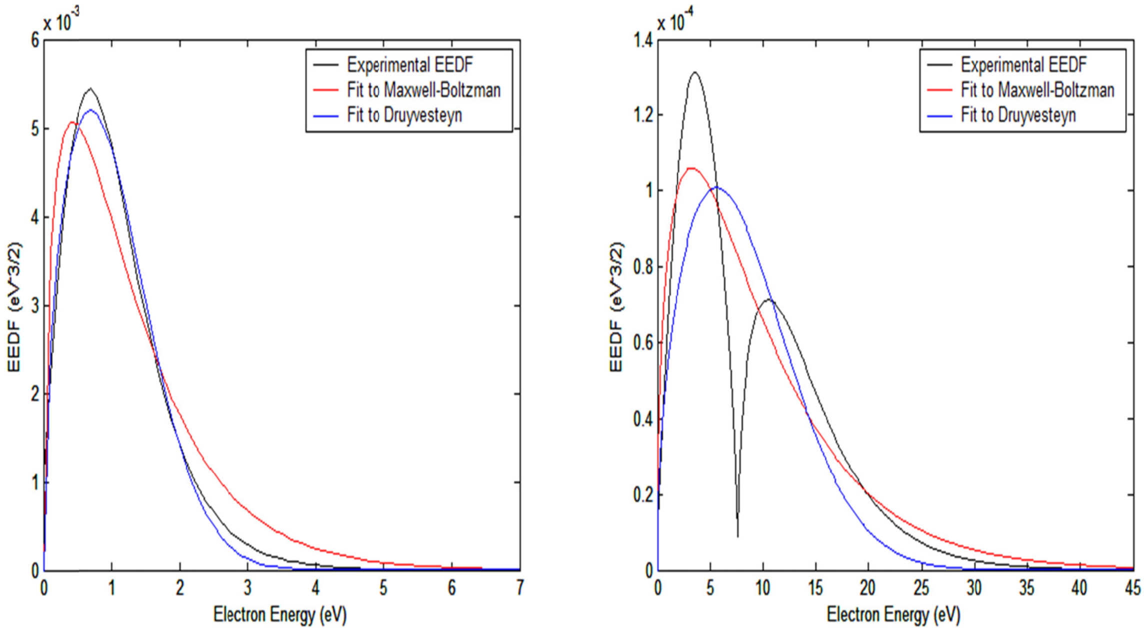

a. P= 5×10^{-2} mbar b. p = 8×10^{-1} mbar

Figure 14. (EEDFs) obtained using fitted method at two pressures

Figure 14 show the experimental (EEDFs) and the fitting to Maxwell and Druyvesteyn distributions functions at two different pressures. The plot indicates that(EEDFs) have a good fitting with the Druyvesteyn distributions and deviates from the Maxwell distributions at low pressure, P= 5×10^{-2} (mbar).This explains that the Druyvesteyn distributions gives good results of (EEDFs) and is a best applicable distribution function at low pressure. While at higher pressure, there is a nearly described distribution function satisfying applicable Maxweelian distribution function at high pressure, where the plasma has local thermal equilibrium (LTE).Also the amplitude of the experimental (EEDFs) peak is higher than the others two distributions. This gave a large number of low electron energies. Furthermore the distributions have two peaks at high pressure. $p = 8\times10^{-1}$ mbar. This represents two groups of electrons with different energies. The electrons in the first group, low electrons energies, affect local electron densities and local plasma conductance. The electrons in the second group, with high energy, play the main part in the local excitation and the local ions production (Mansour, El-Sayed, Farag, & Elghazaly, 2013). However both fitted distributions gave one peak.

Figure 15 shows the influence of filament current on (EEDFs) at constant gas pressure, $p = 0.05$ mbar. It is clear from the figure that the amplitude of peaks is decreased with the increase of the filament current. This means that the density of low energy electron within the plasma decreases. This in turn, attributed to the negative space charge that arises near the anode due to more emitted electrons from the filament as explained in section (Electron and Ion Densities).

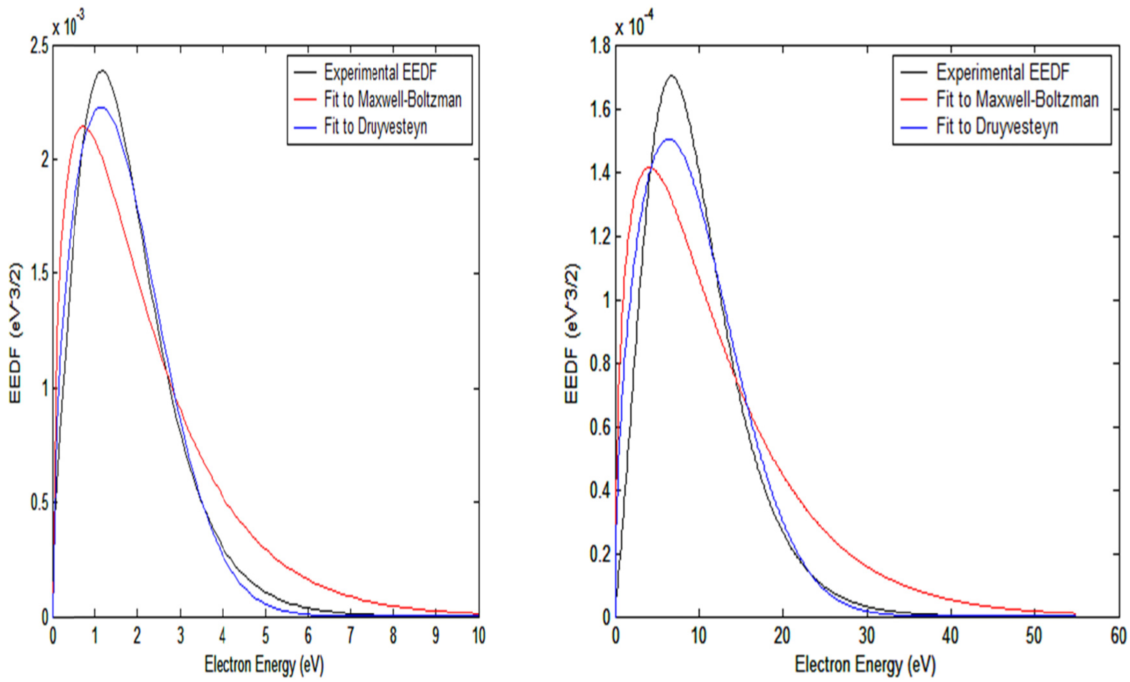

(a) $p = 5\times10^{-2}$ mbar and $I_f = 0.3$ A (b) $p = 5\times10^{-2}$ mbar and $I_f = 1.5$

Figure 15. Electron energy distribution functions at different pressure

4. Conclusions

Hot cathode filament and cylindrical hollow anode DC glow discharge was studied experimentally using single Langmuir probe. From the measured and calculated plasma parameters, important results and conclusions are summarized as follows:

1) The voltage - current characteristics curve of discharge has positive resistance and represents an abnormal glow discharge region of discharge.
2) Increasing of filament current leads to accumulation of negative space charge near the anode.
3) Variation of electron temperature with the filament current closes to the increasing exponential at low pressure investigated.
4) Peaks amplitude of (EEDFs) decreases with the increases of gas pressure, and there is a good fitting with the Druyvesteyn's distribution at low pressure and deviate from Maxwell's distributions function.

5) There are two groups of electrons according to the two peaks of (EEDFs).
6) The amplitude of peaks decrease, with the increases of filament current, this means decreasing the density of low energy electron within the plasma.
7) Peaks amplitude of (EEDFs) obtained using experimental fitting method is higher than both Maxwell's and Druyvesteyn's distribution.

References

Abdelsalam, F. W., Abdelrahman, M. M., Soliman, B. A., Basal, N. I., & Authority, A. E. (2013). Determination of the optimum design and extraction optics for a glow discharge Ion source. *Physical Review & Research International, 3*(4), 425-437.

Azooz, A. A. (2008). Four free parameter empirical parametrization of glow discharge Langmuir probe data. *Review of Scientific Instruments, 79*(10), 103501. http://dx.doi.org/10.1063/1.2976755

Borkhari, A. F., & Yasserian, K. (2013). Influence of the hot filament on the electrical breakdown characteristics in the presence of Ar/N2. *Journal of Theoretical and Applied Physics, 7*(1), 1-5. http://dx.doi.org/10.1186/2251-7235-7-5

Braithwaite, N. S. J. (1990). Electron energy distribution functions in processing plasmas. *Pure and Applied Chemistry, 62*(9), 1721-1728. http://dx.doi.org/10.1351/pac199062091721

Cercek, M., & Gyergyek, T. **(**2004). Structure of a Discharge Plasma with Negative Ions Model and Simulation. *31 st EPS Conferences on Plasma Phys*. London, 28 June-2 July 2004. ECA Vol.28G P-4.228.

Chen, Y., Hu, C., Liu, Z., Xie, Y., Liu, S., & Jiang, C. (2013). Study the Characteristic of the Hot Cathode of High Current Ion Source. *Journal of Fusion Energy, 32*(5), 536-539. http://dx.doi.org/10.1007/s10894-013-9609-x

Ehlers, K. W., & Leung, K. N. (1979). Some characteristics of tungsten filaments operated as cathodes in a gas discharge. *Review of Scientific Instruments, 50*(3), 356-361. http://dx.doi.org/10.1063/1.1135827

Eizaldeen, F. K., & Ashwaq, A. A. O. (2012). Studies The Effect Of Magnetic Field On Argon Plasma Characteristics. *Australian Journal of Basic and Applied Sciences, 6*(3), 817-825.

Flaxer, E. (2011). Programmable smart electron emission controller for hot filament. *Review of Scientific Instruments, 82*(2), 025111. http://dx.doi.org/10.1063/1.3555340

Fritsche, B., Chevolleau, T., Kourtev, J., Kolitsch, A., & Möller, W. (2002). Plasma diagnostic of an RF magnetron Ar/N< sub> 2</sub> discharge. *Vacuum, 69*(1), 139-145. http://dx.doi.org/10.1016/S0042-207X(02)00322-6

Granstedt, E. M., Raitses, Y., & Fisch, N. J. (2008). Cathode effects in cylindrical Hall thrusters. *Journal of Applied Physics, 104*(10), 103302. http://dx.doi.org/10.1063/1.2999343

Griener, W. (1998). *Classical elecrtodynamic*. New York: Springer. http://dx.doi.org/10.1007/978-1-4612-0587-6

Grill, A. (1993). *Cold Plasma in Materials Fabrication From Fundamentals to Applications*. Institute of Electrical and Electronic Engineers, Inc, New York, USA.

Hajy, D. M. (2014). Investigation of hot cathode and hollow anode argon Glow Discharge plasma. M.Sc. Thesis, College of Science, University of Duhok, Iraq.

Handly, W., & Robertson, S. (2009). A Hot- Filament with Very Low Electron Temperature. *Phys, Plasmas,* 16. http://dx.doi.org/10.1063/1.3075935

Jiang, H., Gai, F., Chen, S., Li, X., Chen, J., & Tian, W. (2014). Experimental Study of Electron Gun With Hollow-Anode Vacuum-Arc-Plasma Cathode.

Jomachi, B., & Klobes, B. (2005). *Franck-Hertz Experiment*. Advanced Laboratory Course, University Bonn.

Leshkov, S., Kudrna, P., Chichina, M., & Pickova, I. (2008). *Langmuir Probe Diagnostics of Dc Hollow Cathode Discharge During Tiox Deposition* (pp. 122-126). WDS 08 proceedings of contributed papers, part II.

Lochte-Holtegreven, W. (1968). Plasma-diagnostics. *Amsterdam: North-Holland Publication Co., 1968, edited by Lochte-Holtegreven, W.*, *1*.

Mansour, M. M., El-Sayed, N. M., Farag, O. F., & Elghazaly, M. H. (2013). Effect of He and Ar Addition on N_2 Glow Discharge Characteristics and Plasma Diagnostics. *Arab Journal of Nuclear Science and Applicatins, 46*(1), 116-125. http://dx.doi.org/10.2355/isijinternational.53.1923

Matsuura, M., & Wagatsuma, K. (2013). Two-dimensional Observation of Emission Image of a Copper Chip Excited in a Glow Discharge Plasma. *ISIJ international, 53*(11), 1923-1926.

Miyamoto, N., Imakita, S. H., Kasuya, T., Shimamoto, S., & Wada, M. (2009). Ion Beam Current Characteristic of Bernas -Type Ion Source With a Co-axial Cathode. *J. Plasma Fusion Res. Series, 8*.

Mujawar, M. A. (2013). *Studies on constricted hollow anode plasma source for negative ion production* (Doctoral dissertation, Dublin City University).

Park, H., You, S. J., & Choe, W. (2010). Correlation between excitation temperature and electron temperature with two groups of electron energy distributions. *Physics of Plasmas (1994-present), 17*(10), 103501. http://dx.doi.org/10.1063/1.3486093

Salim, A. J. (2007). *Study the Properties of Glow Discharge Helium Plasma Using Langmuir Single Probe and Data Acquisition System*. M.Sc.Thesis, College of Science,University of Mosul, Iraq.

Shevchenko, E. F., Tarala, V. A., Shevchenko, M. Y., & Titarenko, A. A. (2014). Diamond-Like Carbon Film Deposition Using DC Ion Source with Cold Hollow Cathode. *Advances in Materials Science and Engineering*, 2014. http://dx.doi.org/10.1155/2014/979450

Swarnalatha, M., Sravani, C., Gunasekhar, K. R., Muralidhar, G. K., & Mohan, S. (1997). Estimation of density of charge species in a triode discharge system. *Vacuum, 48*(10), 845-848. http://dx.doi.org/10.1016/S0042-207X (97)00082-1

Tutyk, V. A., Ovcharuk, A. N., Gasik, M. I., & Maslenikov, D. V. (2013). Ignition Features of Plasma-Beam Discharge in Gas-Discharge Electron Gun Operation. *Acta Polytechnica, 53*(2).

Yasserian, K., Borkhari, A. F., & Dorranian, D. (2012). The Electrical Breakdown Characteristics in the Presence of a Hot Filament for Ar and N2 Gases. *World Applied Science Journal, 17*(6), 755-758.

Zhe, F., Zhigang, G., Yikang, P., & Xiaozhang, Z. (2010). Preliminary Investigation on a Sheet Plasma Produced by a Single Hot-Filament Cathode Discharge. *Plasma Science and Technology, 12*(3), 304. http://dx.doi.org/10.1088/1009-0630/12/3/12